Modeling of an Environmentally Independent and Contactless Speed Sensor for Measuring the Speed of Ships, Submarines, and Aircraft in Relation to the Ground Development of Image

Jakaria Mahdi Imam, Mohammad Aminul Islam, Norrima Mokhtar, S. F. W. Muhammad Hatta
Department of Electrical Engineering, Faculty of Engineering, 50603 University of Malaya, Malaysia

Heshalini Rajagopal
Institute of Computer Science and Digital Innovation, UCSI University, 56000 Kuala Lumpur, Malaysia

E-mail: s2133586@um.edu.my, aminul.islam@um.edu.my, norrimamokhtar@um.edu.my ,sh_fatmadiana@um.edu.my

Abstract

We are presenting a theoretical and mathematical model for an environment nondependent contactless speed sensor which can measure directly the horizontal speed of ships, submarines, and aircraft with respect to the ground. Currently, available standalone onboard speed sensors used in ships, submarines, and aircraft measure the speed of the vehicle with respect to the water or air; not ground. Thus, they are unable to measure the ground speed of these vehicles directly. In this paper, we have shown that a novel speed sensor can be designed by using small size dropped inside a vacuum chamber. The theoretical and mathematical model of the proposed sensor was further validated by simulation. The simulation results showed that unlike the conventional methods our proposed method can measure the speed of ships, submarines, and aircraft with respect to the ground directly. Another issue is that current speed sensors are environment-dependent, meaning they or their probes require some type of touch with the operational environment. This environment dependency further affects the accuracy of these sensors, as well as lays these sensors or their probes at risk of collision with external objects. However, the requirement to mount the sensor or its probes outside the vehicle is removed by our suggested sensor. The complete sensor assembly can be placed inside the vehicle.

Keywords: 3D Pose Estimation, Accelerometer, Computer Vision, Free-Fall Ball, Gyro, Inertial Measurement Unit (IMU), Inertial Navigation System (INS), Image Processing, Simultaneous Localization And Mapping (SLAM), Speedometer

1. Introduction

At present ships and submarines use Electromagnetic Log (EM Log), Pitometer Log, and other types of speed sensors for their speed measurement[1][2][3]. But all these sensors measure the speed of the vessel with respect to water, not ground[4]. As a result due to tide or current, vessels can't measure their speed with respect to the ground directly[4]. For example, if a ship is anchored at sea under a strong current, its speed sensor shall show that it is moving at high speed[5], though, in reality, it is standing still with respect to the ground[5]. Similarly, aircraft use the pilot tube for their speed measurement with respect to air, not ground[6], [7]. As a result due to air, aircraft can't measure their speed with respect to the ground directly[8][9][10][11]. For instance, if a helicopter is hovering at zero speed under the heavy wind, its speed sensor shall show that it is moving at high speed[11]. Though in reality, it is standing still with respect to the ground[11].

Fig.1 shows the current method used by ships for ground speed measurement. At present ships measure their ground speed by calculating the EM Log speed information, propeller speed information, wind sensor information, and the Tide Table information[5].

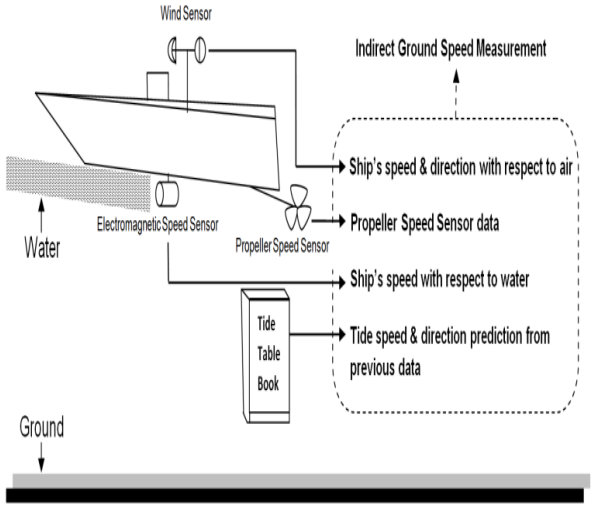

Fig.1.Current method used by ships for ground speed measurement

However, because of faults in the EM Log and Tide Table, this technique yields significant errors in the ground speed measurement[1]. Same way, in the absence of GPS and external sources an aircraft has to measure its ground speed by using air speed, altitude, pressure, density, and other information collected from various onboard sensors. This will also introduce large errors in ground speed measurement due to inaccuracies of input parameters. Though measurement of speed with respect to ground is an important aspect of navigation for water and air vehicles, due to the above reasons ships, submarines, and aircraft cannot measure their ground speed directly. Moreover, currently available speed sensors used in water and air vehicles are environment-dependent; which means these sensors or their probes need some sort of contact with the operating environment. As a result operating environment parameters such as temperature, density, salinity, chemical properties, etc. further affect the accuracy of these sensors. Besides as these sensors or their probes need to be placed outside the vehicle, it initiates further risk of collision with external objects.

GPS is used for speed measurement with respect to the ground, but GPS is not a standalone solution for ships and aircraft as it is susceptible to jamming and spoofing[12][13]. On the other hand, GPS doesn't work when submarines operate underwater[14]. In rare cases, accelerometers are used by vehicles for ground speed measurement[15][16]. In such cases, the inaccuracy in ground speed measurement is increased over time because of numerous sorts of bias, noise, and errors in accelerometer sensors[17]. As the error increases at a large amount with time, they are not used alone; rather they are used with other sensors for measuring ground speed[15][16][17]. To date, no environment non-dependent contactless standalone onboard speed sensor is known to exist, which can measure the speed of water and air vehicles directly with respect to the ground. Hence we proposed a new method of an environment non-dependent contactless standalone onboard speed sensor (just like a standalone Gyro Sensor or Accelerometer Sensor) which can measure the speed of water and air vehicles with respect to the ground directly; without knowing other information such as speed of current, RPM of the propeller, etc.

In this paper, we proposed a new approach for the theoretical and mathematical model of a contactless speed sensor which can measure the speed of the ships, submarines, and aircraft with respect to the ground directly. Another important focus of our approach was to completely eliminate the environmental dependency. The theoretical and mathematical model of the proposed sensor was further validated by simulation.

2. Materials and Methods

2.1. *Theoretical Background*

In 1638, Galileo established the principle of compound motion[18]. According to this principle, in projectile motion the horizontal motion (velocity in x-axis and y-axis) and the vertical motion (velocity in z-axis) are independent of each other; that is, neither motion affects the other. For better understanding let us assume at earth an object is at free fall in an airless environment. According to Galileo the three-axis velocity profile of the object is shown in Table 1[18].

Table 1. Properties of the free-falling object in the airless environment

Time (Sec)	Velocity in x-Axis (m/s)	Velocity in y-Axis (m/s)	Velocity in z-Axis (m/s)
0.1	5	10	0.98
0.2	5	10	1.96
0.3	5	10	2.94
0.4	5	10	3.92
0.5	5	10	4.9
0.6	5	10	5.88
0.7	5	10	6.86
0.8	5	10	7.84
0.9	5	10	8.82
1.0	5	10	9.8

Table 1 shows that if there is no other external resistance on a free-fall object, gravity does not affect the horizontal velocity (x-axis and y-axis velocity) and they remain unchanged over time. Only the vertical velocity (z-axis velocity) is changed over time due to gravity. It means that if we can measure the x-axis and y-axis velocity of the object only once, we know that these two axis velocities shall remain constant until the object touches the ground. This understanding shows the possibility of developing a new sensor by arranging small size free falling balls inside a vacuum chamber for direct measurement of the horizontal velocity (along the x and y-axis) of a vehicle with respect to ground.

2.2. *Description of Device/ Sensor*

Previously it is discussed and shown that currently available speed sensors used in water and air vehicles cannot measure ground speed directly and they need some sort of contact with the operating environment. They need propeller speed information, tide table information, and other information for indirect ground speed measurement Fig.1. Unlike these sensors our proposed speed sensor can measure ground speed directly without any other extra information like propeller speed information, tide table information, etc. and it does not require any sort of contact with the operating environment. It can be placed at any suitable place inside the vehicle Fig.2.

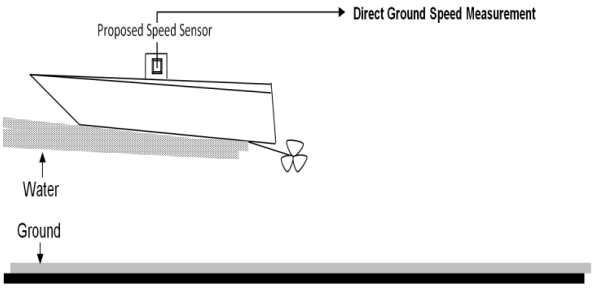

Fig.2.Proposed contactless speed sensor placed inside a ship for direct measurement of ground speed

Fig.3 shows the basic configuration of the proposed speed sensor. The proposed speed sensor consists of an enclosed vacuum chamber. A continuous free-fall ball dropping mechanism is arranged inside this vacuum chamber. Inside the vacuum chamber the balls fall from the top in a single line. Once they reach the bottom of the vacuum chamber, they are again sent to the top. The arrangement is done in such a way that at least 2 balls shall always be at free fall. A 3D Range Finder is placed at the perimeter of the vacuum chamber. The 3D Range Finder is capable of determining the 3D distance of at least 2 free-falling balls at the same time.

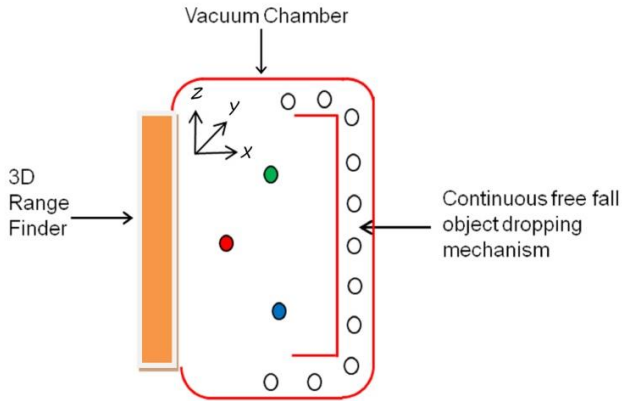

Fig.3.Basic configuration of the sensor

2.3. *Operating Principle*

For better understanding firstly a single free-falling ball is discussed using Fig.4. Subsequently, multiple free-falling balls are discussed using Fig.5.

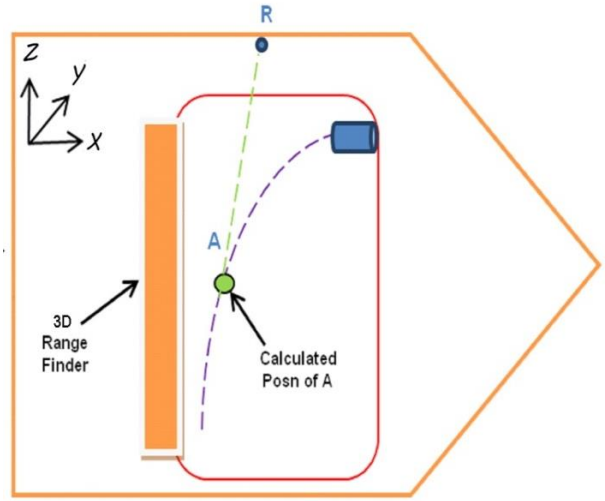

Fig.4.Sensor assembly placed inside a vehicle

During initial set up the sensor assembly is fixed rigidly inside the vehicle. Then it is aligned with the vehicle in all 3 axes. To get the system to work we need to know the 3 axis orientation of the vehicle with respect to earth, Gravity model and the relative distance between the falling ball and the vehicle at all times.

To measure the 3-axis global orientation of the vehicle a 3-axis gyro may be used. To measure the gravity model a 3-axis accelerometer may be used. To measure the relative distance between the falling ball and the vehicle

(point R) a LIDAR, RADAR, SONAR, Stereo Camera, Time of Flight Camera, Kinect, or any other suitable device referred to as 3D Range Finder may be used. When the sensor starts operating, the first ball A starts falling. During free-fall ball A moves at constant velocities along x and y-axes as described in Table 1 with respect to ground until it touches the vacuum chamber. At the beginning of the operation at time t0, we need to know the x and y-axis velocities of falling ball A with respect to ground from external sources (like GPS) only for once. For subsequent operations, the external source shall not be required anymore.

From the understanding of Table 1 once we get the 2 axes' horizontal velocity of the falling ball A at any instance t0, afterward at any moment we can predict its 2 axes' horizontal velocity with respect to ground by simple mathematics without the necessity of any external source/sensor. As a result, the falling ball A can now be used as a reference for speed with respect to ground.

For better understanding let us assume, that just after t0 the vehicle started to move at various speeds and directions. Now if we can measure the relative distance between the falling ball A and the vehicle at 2 different times, then using the falling ball as a reference for speed, we can find out the 2 axes' average horizontal velocity of the vehicle in between these times.

At the end of the free fall when ball A touches the vacuum chamber, it can no longer be used as a reference for speed. But the referencing system must go on for measuring the velocity of the vehicle continuously. To solve this problem a continuous loop of multiple dropping balls (similar to ball A) in a single line is introduced which is shown in Fig.5.

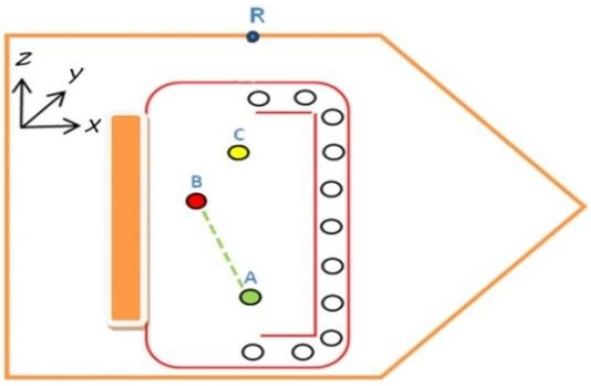

Fig.5.Operation of multiple free-falling balls inside the sensor

The loop shall work in a way so that at least 2 balls shall always be at free fall. As a result after ball A, the next ball B shall start falling. Then the reference shall be shifted from ball A to ball B for determining the 2-axis horizontal velocity of the vehicle. This reference shifting must be done before ball A touches the bottom. Ball B qualifies to be a reference once we find out its 2-axis horizontal velocity. The method of finding out the 2-axis horizontal velocity of ball B is almost similar to the method we found out the 2-axis horizontal velocity of the vehicle. To do this we need to measure the 2 axes (horizontal) relative distance of the falling ball B from falling ball A at 2 different times using the same 3D range finder. Then using the falling ball A as a reference, we can find out the 2-axis horizontal velocity of falling ball B.

Once we know the 2-axis horizontal velocity of ball B, it can be used as a reference instead of ball A. Now ball B can be used in the same manner as ball A for determining the 2 axes' average horizontal velocity of the vehicle. In the same way, the reference shall be subsequently shifted to balls C, D, E, F, G, H, and so on. Fig.6 shows the basic operating principle of the speed sensor in the flowchart.

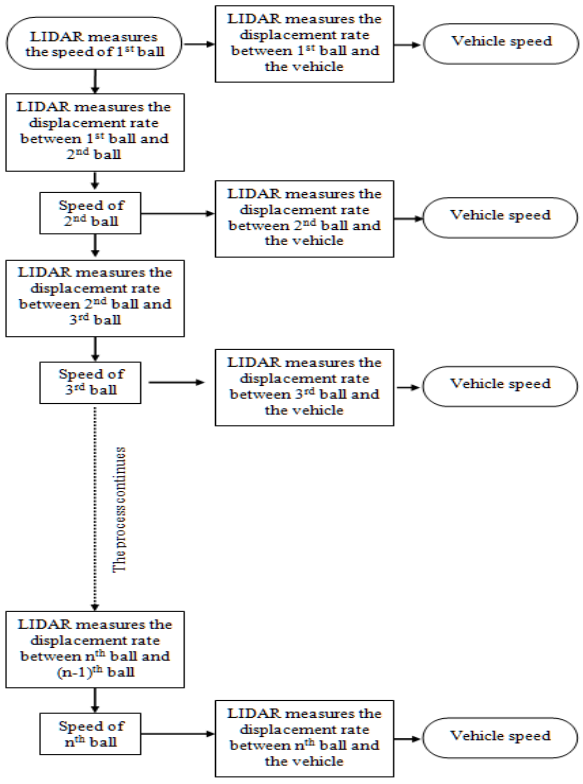

Fig.6.Operating principle of the proposed speed sensor in flowchart

2.4. *Mathematical Modeling*

Table 2 shows the notation used in this work.

Table 2. Notations used in this work

Symbol	Meaning
T	Time (second)
v_{M_x}	Velocity of the current ref ball on x-axis (m/s)
v_{M_y}	Velocity of the current ref ball on y-axis (m/s)
d_{RM_x}	Distance between current ref ball and vehicle ref point R on x-axis (m)
d_{RM_y}	Distance between current ref ball and vehicle ref point R on y-axis (m)
v_{V_x}	Velocity of the vehicle on x-axis (m/s)
v_{V_y}	Velocity of the vehicle on y-axis (m/s)
d_{NM_x}	Distance between current ref ball and next ball on x-axis (m)
d_{NM_y}	Distance between current ref ball and next ball on y-axis (m)
v_{N_x}	Velocity of the next ref ball on x-axis (m/s)
v_{N_y}	Velocity of the next ref ball on y-axis (m/s)

Initially, we know the 2-axis horizontal velocity of the falling ball A. Let us assume we measured its velocity along the x and y-axis as $v_{A_{xt0}}$ and $v_{A_{yt0}}$ respectively at time t0. As long A doesn't touch the bottom, afterward at any time t1 its horizontal velocity can be predicted along the x and y-axis as:

$$v_{A_{xt1}} = v_{A_{xt0}} \quad (1)$$

$$v_{A_{yt1}} = v_{A_{yt0}} \quad (2)$$

In the same way at time t2 , 2 axis horizontal velocity of the falling ball A can be predicted as:

$$v_{A_{xt2}} = v_{A_{xt1}} = v_{A_{xt0}} \quad (3)$$

$$v_{A_{yt2}} = v_{A_{yt1}} = v_{A_{yt0}} \quad (4)$$

Now we need to measure the relative distance of the falling ball A from the vehicle reference point R on the horizontal 2 axes at 2 different times t1 and t2.
Let us assume, we could measure the horizontal 2 axis relative distance of the falling ball A from the vehicle reference point R in the horizontal 2 axes at time t1 and t2 as $d_{RA_{xt1}}$, $d_{RA_{yt1}}$ and $d_{RA_{xt2}}$, $d_{RA_{yt2}}$ respectively. So, in-between time t1 and t2 the 2 axes' average horizontal velocity of the vehicle can be calculated as:

$$v_{V_{x(t1\,\&\,t2)}} = v_{A_{xt2}} - \{d_{RA_{xt2}} - d_{RA_{xt1}}) / (t_2 - t_1)\} \quad (5)$$

$$v_{V_{y(t1\,\&\,t2)}} = v_{A_{yt2}} - \{d_{RA_{yt2}} - d_{RA_{yt1}}) / (t_2 - t_1)\} \quad (6)$$

In the same way we can continue to find out the 2 axis average horizontal velocity of the vehicle in between the times t2 & t3 , t3 & t4 , t4 & t5 , ... , tn-1 & tn and the above equations can be simplified as:

$$v_{A_{xtn}} = v_{A_{xt(n-1)}} \quad (7)$$

$$v_{A_{ytn}} = v_{A_{yt(n-1)}} \quad (8)$$

$$v_{V_{x(tn-1\,\&\,tn)}} = v_{A_{xtn}} - \{(d_{RA_{xtn}} - d_{RA_{xtn-1}})/(t_n - t_{n-1})\} \quad (9)$$

$$v_{V_{y(tn-1\,\&\,tn)}} = v_{A_{xtn}} - \{(d_{RA_{ytn}} - d_{RA_{ytn-1}})/(t_n - t_{n-1})\} \quad (10)$$

Let us assume later at time t6 the next ball B appeared. We measured the 2 axes (horizontal) relative distance of the falling ball B from falling ball A at time t6 as $d_{BA_{xt6}}$, $d_{BA_{yt6}}$ and at time t7 as $d_{BA_{xt7}}$, $d_{BA_{yt7}}$respectively. So, at time t7 the 2 axis horizontal velocity of falling ball B can be calculated as:

$$v_{B_{xt7}} = v_{A_{xt6}} + \{(d_{BA_{xt7}} - d_{BA_{xt6}})/(t_7 - t_6)\} \quad (11)$$

$$v_{B_{yt7}} = v_{A_{yt6}} + \{(d_{BA_{yt7}} - d_{BA_{yt6}})/(t_7 - t_6)\} \quad (12)$$

The above equations can be simplified as:

$$v_{B_{xtn}} = v_{A_{xtn-1}} + \{(d_{BA_{xtn}} - d_{BA_{xtn-1}})/(t_n - t_{n-1})\} \quad (13)$$

$$v_{B_{ytn}} = v_{A_{ytn-1}} + \{(d_{BA_{ytn}} - d_{BA_{ytn-1}})/(t_n - t_{n-1})\} \quad (14)$$

Once we know the 2-axis horizontal velocity of ball B, it can be used as a reference for speed instead of ball A. In the same way, the reference shall be subsequently shifted to balls C, D, E, F, G, H, and so on. Now, if we consider the current reference ball as M and the next reference ball as N, then for a continuous falling ball system, we need to find out the 2-axis horizontal velocity of the next ball from the current ball. In that case, the reference shifting equations can be expressed as:

$$v_{N_{xtn}} = v_{M_{xtn-1}} + \{(d_{NM_{xtn}} - d_{NM_{xtn-1}})/(t_n - t_{n-1})\} \quad (15)$$

$$v_{N_{ytn}} = v_{M_{ytn-1}} + \{(d_{NM_{ytn}} - d_{NM_{ytn-1}})/(t_n - t_{n-1})\} \quad (16)$$

Once we find out the 2-axis horizontal velocity of the next ball, it should be used as the current reference/marker.

At any time the 2 axes horizontal velocity of the current reference of a continuous falling ball system can be predicted as:

$$v_{M_{xtn}} = v_{M_{xtn-1}} \quad (17)$$

$$v_{M_{ytn}} = v_{M_{ytn-1}} \quad (18)$$

For a continuous falling ball system the 2 axis average horizontal velocity of the vehicle can be expressed as:

$$v_{V_{x(tn-1\,\&\,tn)}} = v_{M_{xtn}} - \{(d_{RM_{xtn}} - d_{RM_{xtn-1}})/(t_n - t_{n-1})\} \quad (19)$$

$$v_{V_{y(tn-1\,\&\,tn)}} = v_{M_{ytn}} - \{(d_{RM_{ytn}} - d_{RM_{ytn-1}})/(t_n - t_{n-1})\} \quad (20)$$

3. Results and discussion

A computer simulation was designed by using the software MIT Scratch to validate the theoretical and mathematical model of the proposed sensor. To validate the mathematical equations described in the mathematical modeling section, simulation was done both for static and moving vehicle. All distances were calculated in meter and all velocities were calculated in meter per second (m/s).

In the static test, the simulation was done by placing the sensor assembly inside a vehicle whose velocity was zero in all three axes. But this velocity information was kept hidden from the sensor. Simulation results of the Static Test are shown in Table 3.

In the dynamic test, the simulation was done by placing the sensor assembly inside a vehicle that had a constant velocity 5 of m/s on the x-axis and 10 m/s on the y-axis. But this velocity information was kept hidden from the sensor. Simulation results of the Dynamic Test are shown in Table 4.

During the static test, the sensor could successfully find out the velocity of the vehicle as 0 m/s on the x-axis and 0 m/s on the y-axis at all times by using eqn. 19 and 20 respectively. These results are shown in v_{V_x} and v_{V_y} columns of Table 3 respectively.

During the dynamic test, the sensor could successfully find out the velocity of the vehicle as 5 m/s on the x-axis and 10 m/s on the y-axis at all times by using eqn. 19 and 20 respectively. These results are shown in v_{V_x} and v_{V_y} columns of Table 4 respectively. The dynamic test was done multiple times for a vehicle moving at different constant velocities. During each test, vehicle velocities were kept hidden from the sensor. In all cases, the sensor could successfully find out the velocity of the velocity correctly.

The simulation results showed that theoretically, the proposed sensor is capable of measuring the water and air vehicle speed with respect to the ground directly. Unlike conventional sensors, the proposed sensor completely eliminates the requirement for putting the sensor or its probes keeping outside the vehicle. The complete sensor assembly can be placed inside the vehicle. As a result, in comparison with currently available speed sensors, it may provide higher safety in case of collision with external objects. The proposed sensor is contactless and environment nondependent. As a result, unlike conventional sensors, its accuracy shall not be affected by environmental parameters like temperature, density, salinity, chemical properties, etc. The computer simulation was designed based on ideal physics and math equations. But in the real world, these results may vary. To overcome this limitation the proposed sensor needs to be investigated with practical experimentation.

4. Conclusion

Presently available speed sensors used in ships, submarines, and aircraft cannot measure the vehicle speed with respect to the ground directly. We proposed a theoretical model for a new speed sensor that can measure the horizontal speed of water and air vehicles with respect to the ground directly. The model has also been validated by designing a computer simulation. The simulation results showed that the proposed sensor is capable of measuring the water and air vehicle speed with respect to the ground directly. Unlike the conventional sensors, our proposed sensor is environmentally independent. It completely eliminates the requirement of putting the sensor or its probes outside the vehicle. The complete sensor assembly can be placed inside the vehicle. The proposed sensor is restricted in some aspects because we assume an ideal behavior of the falling balls in an airless environment. This limitation has to be investigated experimentally. If further experiments show good results a completely new type of speed sensor may be introduced which shall be able to measure the speed of water and air vehicles with respect to the ground directly. As well as it has the potential to provide better accuracy, safety, and applicability than currently available speed sensors used in water and air vehicles.

Table 3. Simulation results of the static test

Sample No.	***T* (s)**	v_{M_x} **(m/s)**	v_{M_y} **(m/s)**	d_{RM_x} **(m) (15)**	d_{RM_y} **(m)**	v_{V_x} **(m/s)**	v_{V_y} **(m/s)**	d_{NM_x} **(m)**	d_{NM_y} **(m)**	v_{N_x} **(m/s)**	v_{N_y} **(m/s)**	***Observation***
					1st Ball is used as a reference							
1	0.1	10	10	1	1	0	0					
2	0.2	10	10	2	2	0	0					
3	0.3	10	10	3	3	0	0					
4	0.4	10	10	4	4	0	0					
5	0.5	10	10	5	5	0	0	4	4			2nd Ball appeared
6	0.6	10	10	6	6	0	0	4	4	10	10	
7	0.7	10	10	7	7	0	0	4	4	10	10	
8	0.8	10	10	8	8	0	0	4	4	10	10	
9	0.9	10	10	9	9	0	0	4	4	10	10	
					2nd Ball is used as a reference as 1st Ball is lost							
10	1.0	10	10	6	6	0	0					
11	1.1	10	10	7	7	0	0	6	6			3rd Ball appeared
12	1.2	10	10	8	8	0	0	6	6	10	10	
13	1.3	10	10	9	9	0	0	6	6	10	10	
					3rd Ball is used as a reference as 2nd Ball is lost							
14	1.4	10	10	4	4	0	0					
15	1.5	10	10	5	5	0	0	4	4			4th Ball appeared
16	1.6	10	10	6	6	0	0	4	4	10	10	
17	1.7	10	10	7	7	0	0	4	4	10	10	
18	1.8	10	10	8	8	0	0	4	4	10	10	
19	1.9	10	10	9	9	0	0	4	4	10	10	
					4th Ball is used as a reference as 3rd Ball is lost							
20	2.0	10	10	6	6	0	0					
21	2.1	10	10	7	7	0	0	6	6			5th Ball appeared
22	2.2	10	10	8	8	0	0	6	6	10	10	
23	2.3	10	10	9	9	0	0	6	6	10	10	
					5th Ball is used as a reference as 4th Ball is lost							
24	2.4	10	10	4	4	0	0					
25	2.5	10	10	5	5	0	0	4	4			6th Ball appeared
26	2.6	10	10	6	6	0	0	4	4	10	10	
27	2.7	10	10	7	7	0	0	4	4	10	10	
28	2.8	10	10	8	8	0	0	4	4	10	10	
29	2.9	10	10	9	9	0	0	4	4	10	10	
					6th Ball is used as a reference as 5th Ball is lost							
30	3.0	10	10	6	6	0	0					
31	3.1	10	10	7	7	0	0	6	6			7th Ball appeared
32	3.2	10	10	8	8	0	0	6	6	10	10	
33	3.3	10	10	9	9	0	0	6	6	10	10	
					7th Ball is used as a reference as the 6th Ball is lost							
					.							
					.							
					.							
					nth Ball is used as reference when (n-1)th Ball is lost							

Table 4. Simulation results of the dynamic test

Sample No.	***T* (s)**	v_{M_x} ***(m/s)***	v_{M_y} ***(m/s)***	d_{RM_x} ***(m)*** **(15)**	d_{RM_y} ***(m)***	v_{V_x} ***(m/s)***	v_{V_y} ***(m/s)***	d_{NM_x} ***(m)***	d_{NM_y} ***(m)***	v_{N_x} ***(m/s)***	v_{N_y} ***(m/s)***	***Observation***
					1st Ball is used as a reference							
1	0.1	15	20	1	1	5	10					
2	0.2	15	20	2	2	5	10					
3	0.3	15	20	3	3	5	10					
4	0.4	15	20	4	4	5	10					
5	0.5	15	20	5	5	5	10	4	4			2nd Ball appeared
6	0.6	15	20	6	6	5	10	4	4	15	20	
7	0.7	15	20	7	7	5	10	4	4	15	20	
8	0.8	15	20	8	8	5	10	4	4	15	20	
9	0.9	15	20	9	9	5	10	4	4	15	20	
					2nd Ball is used as a reference as 1st Ball is lost							
10	1.0	15	20	6	6	5	10					
11	1.1	15	20	7	7	5	10	6	6			3rd Ball appeared
12	1.2	15	20	8	8	5	10	6	6	15	20	
13	1.3	15	20	9	9	5	10	6	6	15	20	
					3rd Ball is used as a reference as 2nd Ball is lost							
14	1.4	15	20	4	4	5	10					
15	1.5	15	20	5	5	5	10	4	4			4th Ball appeared
16	1.6	15	20	6	6	5	10	4	4	15	20	
17	1.7	15	20	7	7	5	10	4	4	15	20	
18	1.8	15	20	8	8	5	10	4	4	15	20	
19	1.9	15	20	9	9	5	10	4	4	15	20	
					4th Ball is used as a reference as 3rd Ball is lost							
20	2.0	15	20	6	6	5	10					
21	2.1	15	20	7	7	5	10	6	6			5th Ball appeared
22	2.2	15	20	8	8	5	10	6	6	15	20	
23	2.3	15	20	9	9	5	10	6	6	15	20	
					5th Ball is used as a reference as 4th Ball is lost							
24	2.4	15	20	4	4	5	10					
25	2.5	15	20	5	5	5	10	4	4			6th Ball appeared
26	2.6	15	20	6	6	5	10	4	4	15	20	
27	2.7	15	20	7	7	5	10	4	4	15	20	
28	2.8	15	20	8	8	5	10	4	4	15	20	
29	2.9	15	20	9	9	5	10	4	4	15	20	
					6th Ball is used as a reference as 5th Ball is lost							
30	3.0	15	20	6	6	5	10					
31	3.1	15	20	7	7	5	10	6	6			7th Ball appeared
32	3.2	15	20	8	8	5	10	6	6	15	20	
33	3.3	15	20	9	9	5	10	6	6	15	20	
					7th Ball is used as a reference as the 6th Ball is lost							
					.							
					.nth Ball is used as reference when (n-1)th Ball is lost							

References

1. Griswold, W. Lyman, "Underwater logs," Navigation: Journal of the Institute of Navigation, vol. 15, no. 2, pp. 127-135, Summer 1968.
2. C. G. Smith, and j. Slepian, "Electromagnetic ship's log," U.S. Patent 1249530, Dec. 11, 1917.
3. R. J. Paredes, Quintuña, M. T. M. Arias-Hidalgo and R. Datla, "Numerical flow characterization around a type 209 submarine using OpenFOAM" Fluids, vol. 6, no. 2, pp. 1-23, Feb. 2021, Art. No. 66.
4. The American Practical Navigator: Bowditch, Paradise Cay Publications, Bethesda, MD, USA, 2010.
5. P. Gloaguen, M. Woillez, S. Mahévas, Y. Vermard, and E. Rivot, "Is speed through water a better proxy for fishing activities than speed over ground," Aquatic Living Resources, vol. 29, no. 2, pp. 1-8, Oct. 2016, Art. No. 210.
6. J. Mcorlly, "Pilot Tube," U.S. Patent 2399370, Apr. 30, 1946.
7. Mechanics of flight, Pearson Education Limited, Harlow, ESX, UK, 2006.
8. Principles Of Flight: Aircraft General Knowledge, Flight Performance and Planning (Private Pilot's Licence Course), Airplan Flight Equipment Ltd, Wythenshawe, MCR, UK, 2005.
9. Tietjens, O.K.G. & Prandtl, L. 1957 Applied Hydro and Aeromechanics: Based on Lectures of L. Prandtl, vol. 2. Courier Corporation.
10. Fluid Flow Handbook, McGraw-Hill Professional, Blacklick, OH, USA, 2002.
11. W. Gracey, "Measurement of aircraft speed and altitude," NASA Langley Research Center, Hampton, VA, USA, Rep No. NASA-RP-1046, May 1, 1980.
12. A. Pinker and C. Smith, "Vulnerability of the GPS Signal to Jamming," GPS Solutions, vol. 29, no. 2, pp. 1-8, Oct. 2016, Art. No. 210.
13. A. Grant, P. Williams, N. Ward and S. Basker, "GPS jamming and the impact on maritime navigation,". The Journal of Navigation, vol. 62, no. 2, pp. 173-187, Apr. 2009.
14. G. Taraldsen, T. A. Reinen and T. Berg, "The underwater gps problem," presented at the Conf. Oceans 2011 IEEE, Spain, Jun. 6-9, 2011.
15. G. Xu, Y. Zhao, K. Xu, H. Xu and Z. Cheng, "A speed measurement method for underwater vehicle based on pulse speedometer and accelerometer," presented at the 23rd Int Conf. Offshore and Polar Engineering, Anchorage, Alaska, Jun. 30 - Jul. 5, 2013.
16. Hwang, J. K., Uchanski, M. and Song, C. K. (2005). Vehicle speed estimation based on Kalman filtering of accelerometer and wheel speed measurements. Int. J. Automotive Technology 6, 5, 475–481.
17. A. Lawrence, "Gyro and accelerometer errors and their consequences," in Modern Inertial Technology, New York, NY, USA: Springer, 1998, pp. 25-42.
18. S. Drake and J. Mclachlan, "Galileo's discovery of the parabolic trajectory," Scientific American, vol. 232, no. 3, pp. 102-111, Mar. 1975.

Authors Introduction

Jakaria Mahdi Imam

He received his B.Eng. degree from Military Institute of Science and Technology, Bangladesh. Currently, he is pursuing master degree by research from University of Malaya, Malaysia. His research interest includes emerging naval technologies, inertial navigation system and inertial sensors.

Dr. Mohammad Aminul Islam

He received M.Sc. (research) and Ph.D. degree in Electrical, Electronic, and System Engineering from the National University of Malaysia (UKM), Malaysia, in 2012 and 2015. He is currently a Senior Lecturer in the Department of Electrical Engineering, University of Malaya. His research interests are semiconductor materials, optical materials and energy transportation.

Dr. Norrima Mokhtar

She received the B.Eng. degree from University of Malaya, the M.Eng. and the Ph.D. degree from Oita Univerity, Japan. She is currently a Senior Lecturer in the Department of Electrical Engineering, University of Malaya. Her research interests are signal processing and human machine interface.

Dr. S. F. W. Muhammad Hatta

She received her M.Eng. in Electrical Electronics Engineering (University of Sheffield, UK) in 2005, M.Sc. in Microelectronics (University of Malaya) in 2009 and Ph.D. in Microelectronics (LJMU,UK) in 2014. She is currently a Senior Lecturer in the Department of Electrical Engineering, University of Malaya. Her research interests include emerging technologies in wearable electronics, semiconductor reliability, advanced semiconductor modelling and characterisation as well as PUF-based technology in cyber-securities.

Dr. Heshalini Rajagopal

She received her PhD and Master's degree from the Department of Electrical Engineering, University of Malaya, Malaysia in 2021 and 2016, respectively. She received the B.E (Electrical) in 2013 Currently, she is an Assistant Professor in UCSI University, Kuala Lumpur, Malaysia. Her research interest includes image processing, artificial intelligence and machine learning.